SUPPLEMENTAL FIGURES

Supplemental figure 1

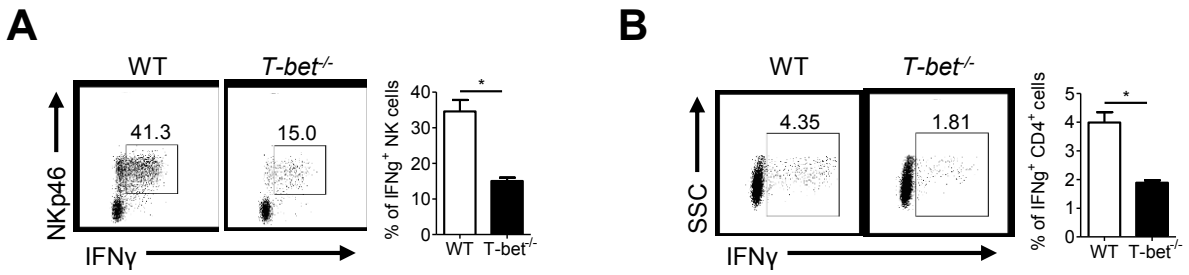

Supplemental Figure 1: IFNγ production is reduced in NK and $CD4^+$ T cells from T-bet deficient mice, Related to Figure 1.

Representative plots and percentage of IFNγ-producing A) NK cells and B) T cells in the spleen of WT and $T\text{-}bet^{-/-}$ mice. NK cells are defined as $CD4^-$ $NK1.1^+$ $NKp46^+$ cells. T cells are gated as $CD4^+$ cells. Data are expressed as mean ± SEM and are representative of at least three independent experiments (n=3). *$p < 0.05$.

Supplemental figure 2

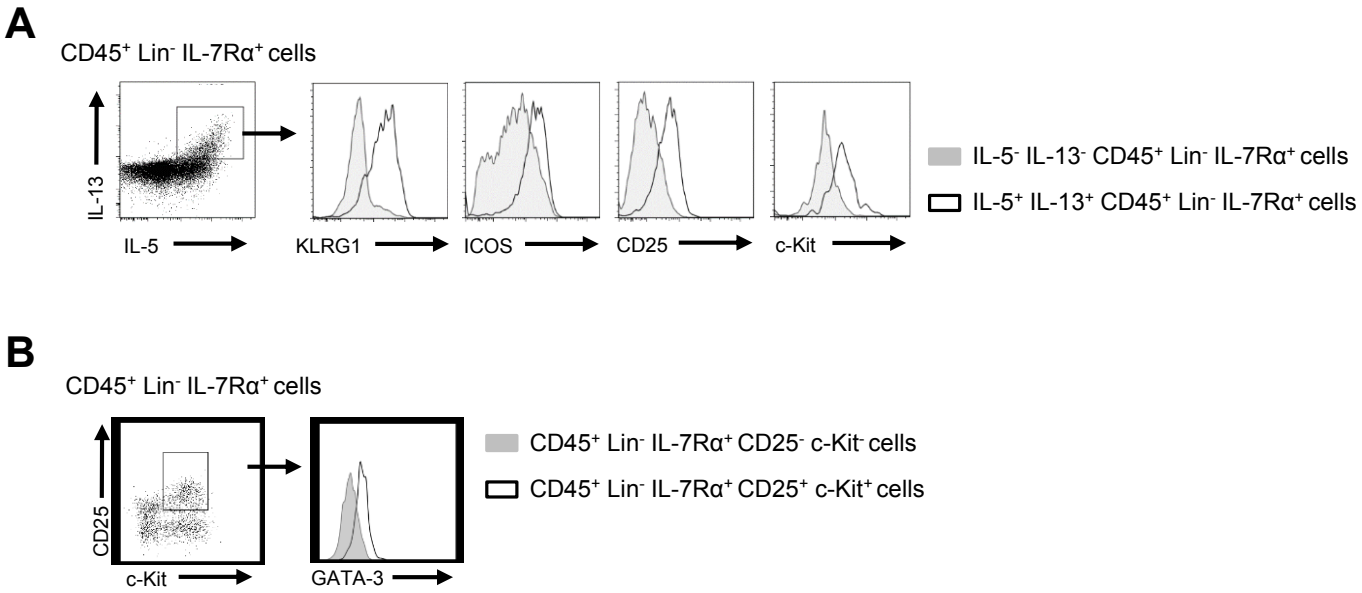

Supplemental Figure 2: Characterisation of surface markers expressed by ILC2s, Related to Figure 1.

Representative plot and histograms showing: A) the expression of surface markers in IL-5 and IL-13 producing ILCs in comparison with IL-5$^-$ IL-13$^-$ ILCs isolated from the cLP of WT mice and stimulated with PMA (50 ng/ml) and ionomycin (1 μg/ml) and ionomycin for 4h prior to intracellular cytokine and surface markers staining; B) GATA-3 expression in CD25$^+$ c-Kit$^+$ ILCs from the spleen of T-bet$^{-/-}$ mice. ILCs are defined as CD45$^+$ Lin$^-$ IL-7Rα$^+$ cells.

Supplemental figure 3

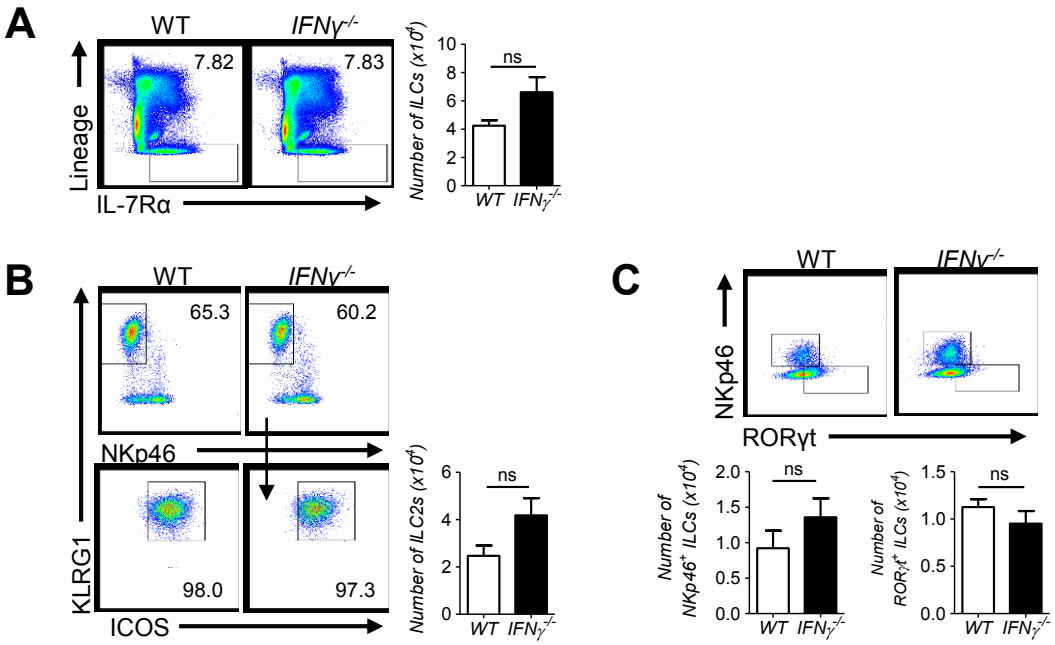

Supplemental Figure 3: Lack of IFNγ is not linked to an expansion of ILC2s, Related to Figure 1.

A-B) Flow cytometry analysis of the different ILC populations in the cLP of WT and IFNγ$^{-/-}$ mice showing: A) Representative plots showing the ILC population within CD45^{+} cells and absolute cell numbers of ILCs; B) Representative plots and absolute cell numbers of KLRG1^{+}ICOS^{+} NKp46^{-} ILCs; C) Representative plots and absolute cell numbers of NKp46^{+} and NKp46^{-} RORγt^{+} ILCs. ILCs are defined as CD45^{+}Lin^{-}IL-7Rα^{+} cells; ILC2s are defined as CD45^{+}Lin^{-}IL-7Rα^{+}ICOS^{+}KLRG1^{+} cells. Data are expressed as mean ± SEM (n=3). ns: non-significant.

Supplemental figure 4

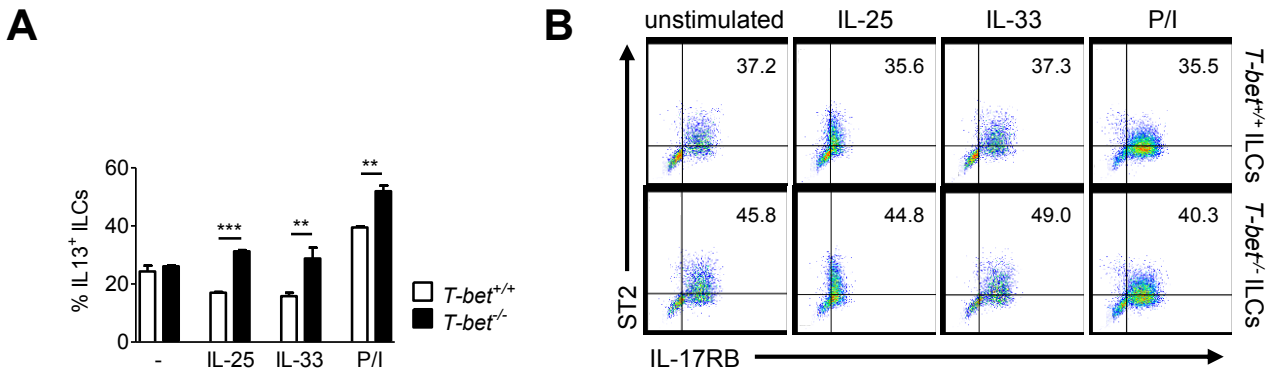

Supplemental Figure 4: ST2 and IL-17RB expression in T-bet$^{+/+}$ and T-bet$^{-/-}$ ILCs, Related to Figure 1.

A) Percentage of IL-13^{+} ILCs and B) representative flow cytometry plots showing expression of ST2 and IL-17RB in IL-13^{+} ILCs from the cLP of T-bet$^{+/+}$ and T-bet$^{-/-}$ mice at baseline (-, unstimulated) and after 4h of stimulation with IL-25 (50ng/ml), IL-33 (50ng/ml), or PMA (50 ng/ml) and ionomycin (1 µg/ml) (P/I). ILCs were defined and FACS-sorted CD45^{+}Lin^{-}IL-7Rα^{+} cells.

Supplemental figure 5

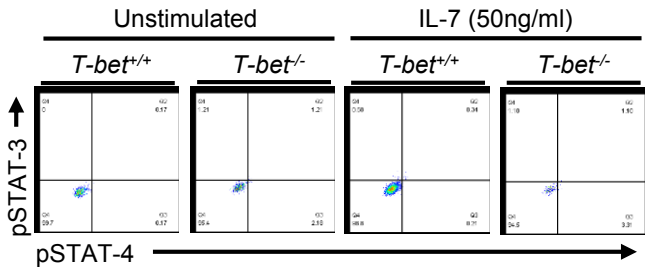

Supplemental Figure 5: STAT-3 and STAT-4 activation in ILCs in response to IL-7 is not altered in the absence of T-bet, Related to Figure 3.

Representative flow cytometry analysis of the phosphorylation of STAT-3 and STAT-4 in ILCs from the cLP of WT and T-bet$^{-/-}$mice after stimulation with IL-7 (50ng/ml, 60 minutes). Data are expressed as mean ± SEM (n=3). ILCs were defined as CD45^{+}Lin^{-}IL-7Rα^{+} cells.

Supplemental figure 6

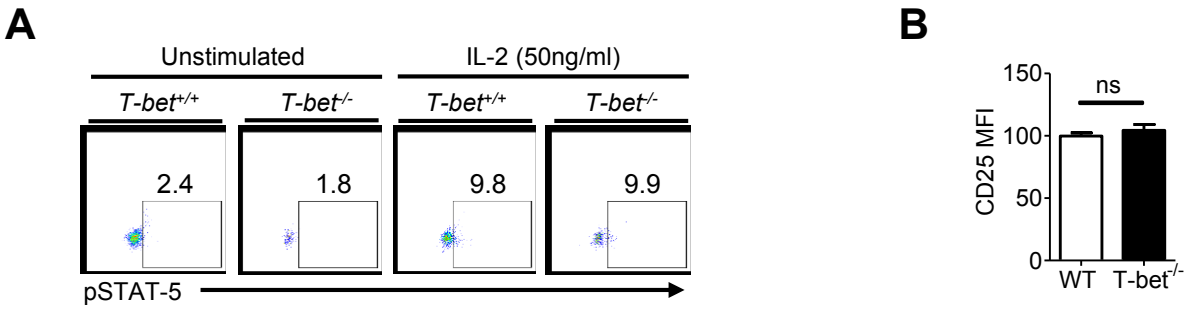

Supplemental Figure 6: IL-2Rα expression and signalling is not altered in ILCs from T-bet deficient mice, Related to Figure 3.

A) Representative flow cytometry analysis of the phosphorylation of STAT5 in ILCs from the cLP of WT and T-bet$^{-/-}$mice after stimulation with IL-2 (50ng/ml, 60 minutes). Numbers indicate percentages.

B) Density of expression of IL-2Rα (CD25) in ILC2s from the cLP of WT and T-bet$^{-/-}$ mice expressed as mean fluorescent intensity (MFI). ILC2s were defined as CD45^{+}Lin^{-}IL-7Rα^{+}KLRG1^{+}ICOS^{+} cells. Data are expressed as mean ± SEM and are representative of at least three independent experiments (n=3). ns= non significant.

Supplemental figure 7

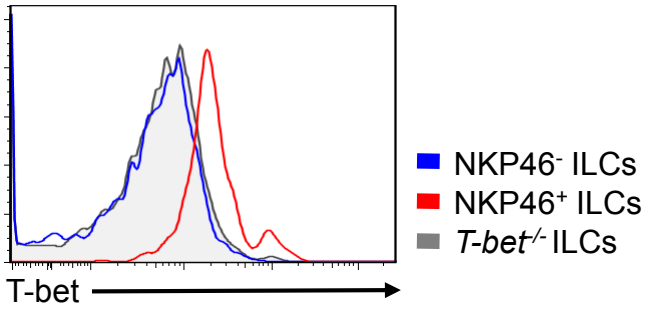

Supplemental Figure 7: Representative histogram showing intracellular staining for T-bet in NKp46^{+} and NKp46^{-} ILCs from WT mice and in ILCs from *T-bet*$^{-/-}$ mice. ILCs are defined as CD45^{+} Lin^{-} IL-7Rα^{+} cells. Related to Figure 5.

Supplemental figure 8

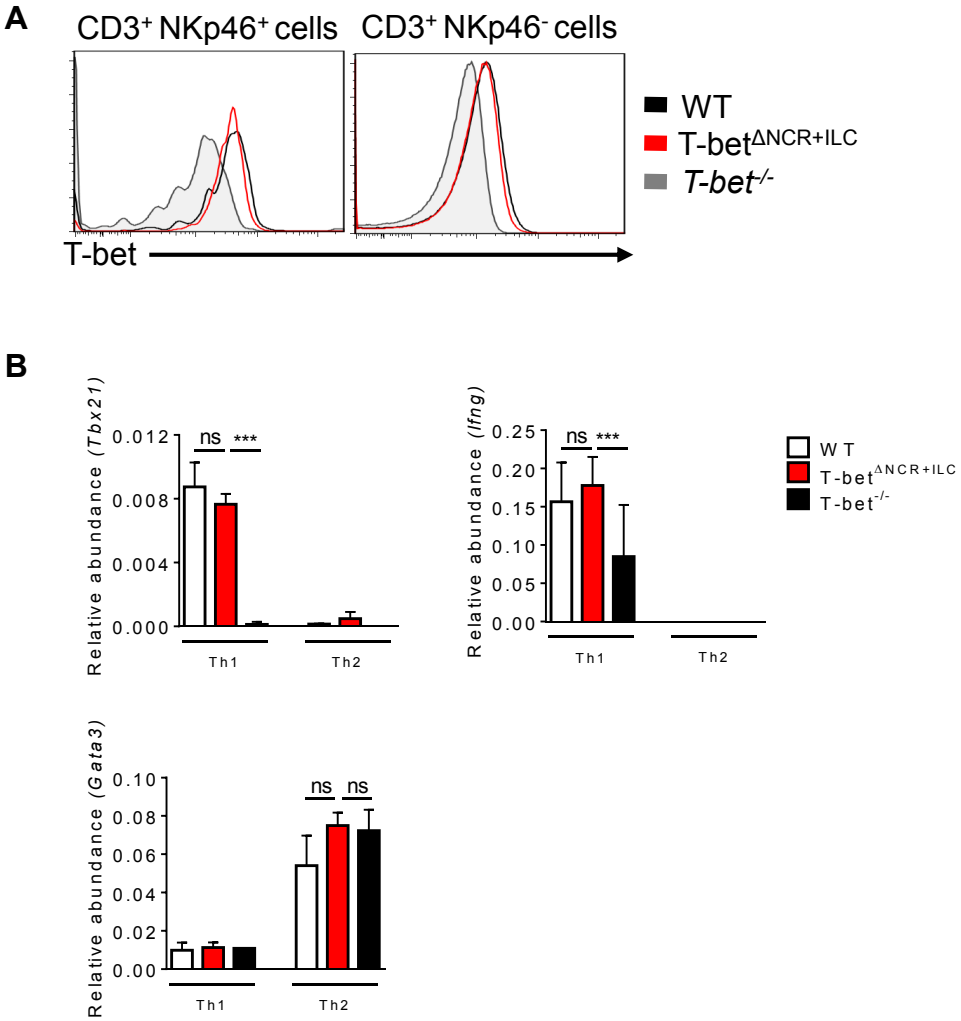

Supplemental Figure 8: T-bet Expression in T cells from the T-bet$^{\Delta NCR+ILC}$ mouse is Not Altered, Related to Figure 5.

A) Representative histogram showing intracellular staining for T-bet in NKp46^{+} and NKp46^{-} CD3^{+} cells from WT, *T-bet*$^{-/-}$ and T-bet$^{\Delta NCR+ILC}$ mice. B) Real-time PCR measuring the transcripts of *Tbx21*, *Ifng* and *Gata3* in Th1 and Th2 in vitro differentiated cells from the spleen of WT, *T-bet*$^{-/-}$ and T-bet$^{\Delta NCR+ILC}$ mice (n=3). Fold change expressed as mean ± SEM *vs.* T-bet$^{\Delta NCR+ILC}$.

Data are expressed as mean ± SEM and are representative of at least three independent experiments. ns: non-significant; ***p<0.001.

Supplemental figure 9

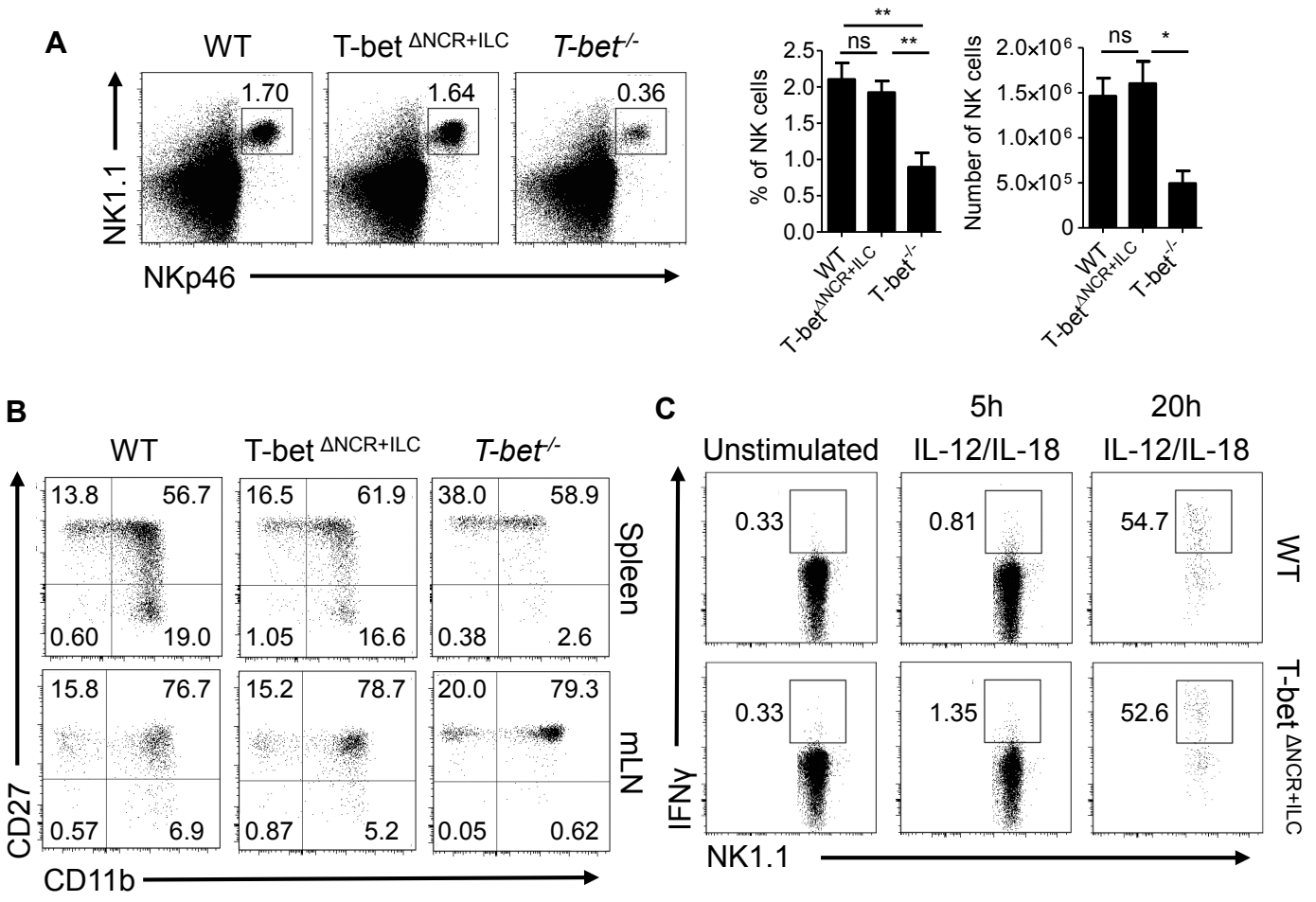

Supplemental Figure 9: Maturation and IFNγ Production by NK Cells from T-bet$^{\Delta NCR+ILC}$ mice are Not Affected by the Absence of T-bet, Related to Figure 5.

Representative flow cytometry plots showing the percentage of NK cells in the spleen of WT, T-bet$^{\Delta NCR+ILC}$ and *T-bet*$^{-/-}$ mice. Percentage and absolute cell numbers (n=3) of NK cells in the spleen of the different mouse strains. B) Representative flow cytometry plots showing the percentages of CD11b^{hi}CD27^{hi} NK cells in the spleen of WT, T-bet$^{\Delta NCR+ILC}$ and *T-bet*$^{-/-}$ mice. C) Representative flow cytometry plots showing intracellular staining for IFNγ in unstimulated splenic NK cells from WT and T-bet$^{\Delta NCR+ILC}$ mice and after stimulation with IL-12 and IL-18 for 5 and 20 hours.

Data are expressed as mean ± SEM and are representative of at least three independent experiments. ns: non-significant; *p < 0.05; **p< 0.01.

Supplemental figure 10

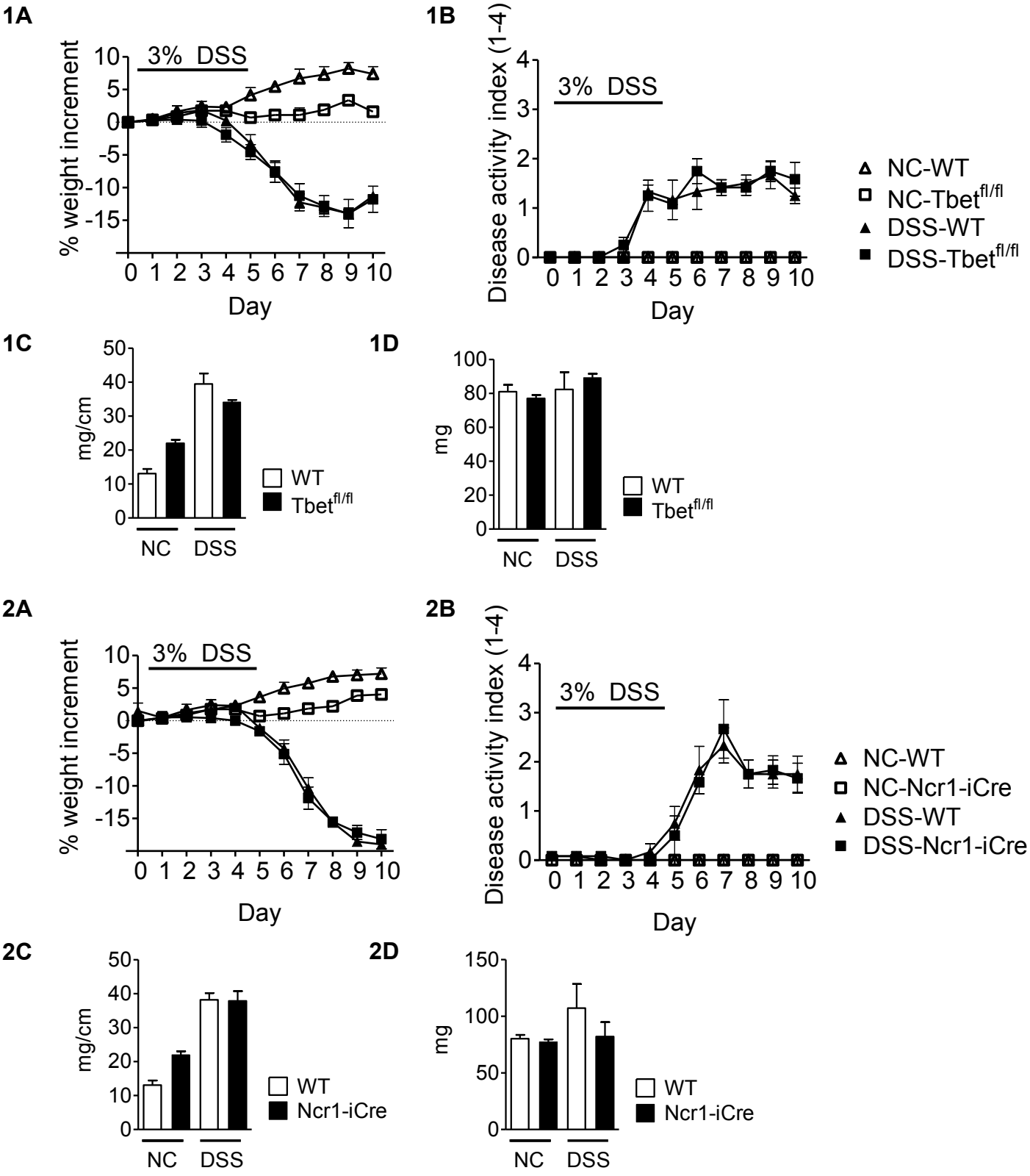

Supplemental Figure 10: *Ncr1*-iCre^{Tg} and *T-bet*$^{fl/fl}$ mice Develop DSS-Colitis Comparable to WT mice, Related to Figure 7.

Panels 1A-D show DSS-colitis phenotype in WT and *T-bet*$^{fl/fl}$ mice. Panels 2A-D show DSS-colitis phenotype in WT and *Ncr1*-iCre^{Tg} mice. A) Weight increment (%) and B) Disease activity index (DAI) values over the 10-day experimental period; C) Colon weight/length ratio and D) Spleen weight. NC represent Non-colitic mice, DSS represent DSS-treated mice. DAI values were calculated based on the criteria proposed previously (Cooper et al., 1993). Data are expressed as Mean +/- SEM (n=4).